HHS Public Access

Author manuscript

Acta Biomater. Author manuscript; available in PMC 2017 November 01.

Published in final edited form as:

Acta Biomater. 2017 March 15; 51: 279–293. doi:10.1016/j.actbio.2017.01.058.

Tuning cell adhesive properties via layer-by-layer assembly of chitosan and alginate

Joana M. Silva[1,2], **José R. García**[3,4], **Rui L. Reis**[1,2], **Andrés J. García**[3,4], and **João F. Mano**[1,2,*,#]

[1]3B's Research Group – Biomaterials, Biodegradables and Biomimetics, University of Minho, Headquarters of the European Institute of Excellence of Tissue Engineering and Regenerative Medicine, Avepark – Parque de Ciência e Tecnologia, Zona Industrial da Gandra, 4805-017 Barco GMR, Portugal

[2]ICVS/3B's -PT Government Associate Laboratory, 4710-243 Braga/Guimarães, Portugal

[3]Petit Institute for Bioengineering and Bioscience, Georgia Institute of Technology, Atlanta, GA 30332, USA

[4]Woodruff School of Mechanical Engineering, Georgia Institute of Technology, Atlanta, GA 30332, USA

Abstract

Understanding the mechanisms controlling cell-multilayer film interactions is crucial to the successful engineering of these coatings for biotechnological and biomedical applications. Herein, we present a strategy to tune the cell adhesive properties of multilayers based on marine polysaccharides with and without cross-linking and/or coating with extracellular matrix proteins. Chemical cross-linking of multilayers improved mechanical properties of the coatings but also elicited changes in surface chemistry that alter the adhesion of human umbilical vein endothelial cells. We evaluated a strategy to decouple the mechanical and chemical properties of these films, enabling the transition from cell-adhesive to cell-resistant multilayers. Addition of chitosan/alginate multilayers on top of cross-linked films decreased endothelial cell adhesion, spreading, and proliferation to similar levels as uncross-linked films. Our findings highlight the key role of surface chemistry in cell-multilayer film interactions, and these engineered nanocoatings represent a tunable model of cell adhesive and non-adhesive multilayered films.

Keywords

surface chemistry; cross-linking; cell adhesion; fibronectin; tissue engineering

*Corresponding author. jmano@ua.pt.

#Current address: Department of Chemistry, CICECO - Aveiro Institute of Materials University of Aveiro 3810-193 Aveiro, Portugal.

Supporting information

Supplementary data associated with this article can be found at free of charge via the Internet.

Introduction

Layer-by-layer (LbL) assembly can produce hierarchical films with fine and precise control over the film properties.[1–7] Since its discovery, LbL assembly has been shown to be a simple, versatile and elegant bottom-up approach for template-assisted assembly of materials.[4, 8–10] This method is based on the sequential adsorption of multivalent molecules on virtually any type of substrate via electrostatic, non-electrostatic, or a combination of thereof.[2, 11–13] The overall properties of the film can be controlled simply by adjusting processing parameters: nature of polyelectrolytes, functional groups, molecular weight, charge density, concentration of the adsorption species, adsorption and rising time, pH, ionic strength, and humidity.[14–19]

By using LbL assembly, an unprecedented variety of different components (i.e. hundreds of different materials) can be used. The nature and intrinsic properties of the building blocks dictate the bulk properties of the film.[2, 4, 20] Natural origin polymer-based multilayers have received particular attention due to their ability to impart unique properties to the polyelectrolyte multilayers (PEMs), such as cytocompatibility, biodegradability, presence of cell recognition sites, and natural similarity to the biological tissues.[21–26] Herein, two polysaccharides were used as polyelectrolytes: chitosan (CHI) and alginate (ALG). Multilayers based on these polysaccharides are stable over a pH range of 3–9, but exhibit high hydration levels and low mechanical strength, which impair cell adhesion.[27–29] Post-assembly modifications can be used to tune these properties, namely adsorption or immobilization of extracellular matrix (ECM) proteins such as laminin (LM) and fibronectin (FN) as well as chemical cross-linking of the films.

Multilayers with poor cell adhesion ability are ideal candidates for an adsorption or chemical attachment of an ECM layer. The kinetics of protein adsorption is governed by electrostatic interactions and other secondary interactions such as hydrophobic interactions and hydrogen bonding.[30] The advantages of covalent immobilization over the adsorption strategy are that the biomolecules immobilized are not easily removed by physical force (e.g., rinsing) and are robust enough to withstand the possible harsh conditions of *in vivo* exposure.[31] Using this approach, it is also possible to avoid the diffusion of biomolecules along the multilayers, allowing a spatial control over its distribution.[30]

Modulation of mechanical properties is a common approach used to tailor the bulk properties of multilayered films. Different approaches can be used to tune mechanical properties including the incorporation of nanocolloids [32], assembly pH [33], or by using covalent cross-linkers such as glutaraldehyde, [34, 35] 1-ethyl-3-(3-dimethylaminopropyl)-carbodiimide (EDC) in combination with sulfo-N-hydroxysulfo-succinimide (EDC/s-NHS) [36–38] and genipin [29, 39]. Genipin is a naturally derived chemical from the gardenia fruit that has been extensively investigated due to its ability to cross-link amine-containing polymers [40, 41] in diverse systems, including multilayered films [39, 42]. Using genipin as cross-linker, a wide range of films of increased stiffness can be obtained by simply varying the reaction time or the concentration of the cross-linker.[43, 44] Genipin cross-linker, however, is reported to have effects on the wettability and roughness of the film. Thus, upon cross-linking of multilayers with genipin, it is challenging to decouple the mechanical and

chemical properties of the films. In a previous study, Discher and co-workers achieved the decoupling of both parameters using polyacrylamide gels grafted with increased densities of collagen.[45] In the present work, we performed a systematic study of the cell adhesive properties of CHI/ALG multilayers upon cross-linking and ECM protein adsorption or immobilization (Scheme I). Although the production and characterization of such multilayered films have been reported, to the best of our knowledge, this is the first time that such films have been used to decouple the effects of mechanical and chemical cues on cell adhesion.

Materials and Methods

Production of multilayered films

The multilayers were processed using CHI of medium molecular weight (M_w 150–300 kDa, 90% degree of deacetylation, Heppe Medical Chitosan, Germany) and low viscosity ALG (538 kDa, ~250 cP, ref.71238, Sigma Aldrich, USA). PEMs were constructed by alternately immersing the tissue culture-grade polystyrene substrate (96 well plate, TCPS, Corning, USA) into a polyethylenimine solution (PEI, 0.5 mg mL^{-1}, 0.15 M sodium acetate buffer, pH 5.5) for 10 min, with an intermediate rinsing step of 10 min. Tissue culture plastic coated with PEI presents a positive charge, providing support for the multilayer assembly. The substrates were then immersed in an ALG solution (1 mg mL^{-1}, 0.1 M sodium acetate buffer/0.15 M NaCl, pH 5.5) for 6 min. After rinsing with 0.1 M sodium acetate buffer/0.15 M NaCl (4 min), the same procedure was followed for CHI deposition (1 mg mL^{-1}, 0.1 M sodium acetate buffer/0.15 M NaCl 0.15 M, pH 5.5). Multilayers were generated by repeating the ALG/CHI deposition for five cycles. After buildup, the multilayers were cross-linked with genipin(Wako chemical, USA). Briefly, genipin solutions (0.125 to 5.0 mg mL^{-1}) were prepared by dissolving the adequate amount of lyophilized genipin into dimethyl sulfoxide (DMSO, Sigma Aldrich USA)/sodium acetate buffer (0.15 M NaCl, pH 5.5) mixture (1:4, v/v). The cross-linked films were then rinsed in sodium acetate buffer (0.15 M NaCl, pH 5.5) for 1 h, followed by extensively washing in ultrapure water. Upon studying the behavior of films at different concentrations of cross-linker, the concentration of 3.5 mg mL^{-1} was selected, which corresponds to a cross-linking degree of ≈ 60.5%. After cross-linking the films, another bilayer was added on top of the film.

Protein Immobilization

Human plasma FN (10 μg mL^{-1}, PBS, pH 7.4, Life Technologies, USA) and murine LM-1 (50 μg mL^{-1}, PBS, pH 7.4, Life Technologies, USA) were adsorbed or immobilized on unmodified or cross-linked films with or without an additional bilayer of ALG/CHI post-ECM coating. The procedure used for protein immobilization was based on pilot studies. Briefly, EDC (2.0 mM) and sulfo-NHS (5.0 mM) were used to pre-activate the proteins by reaction with their carboxyl groups. This step was performed for 20 min at room temperature (RT). The protein solution was then added to the multilayered films. After 4 h of incubation, the multilayered films were extensively washed in PBS. TCPS were used as control surfaces.

Quartz crystal microbalance with dissipation monitoring

The buildup of PEMs was followed *in situ* by quartz crystal microbalance (QCM-Dissipation, Q-Sense, Sweden) using gold-coated sensors excited at the several overtones (25, 35, 45, 55 MHz). The conditions used for the assembly were optimized in previous work.[43, 46] The crystals were cleaned in an ultrasound bath at 30°C using successive acetone, ethanol and isopropanol washes. Exposure of freshly prepared polyelectrolyte solutions (1 mg mL^{-1}) was performed at a constant flow rate of 100 μL min^{-1}. An initial layer of PEI (0.5 mg mL^{-1}, sodium acetate buffer 0.15 M, pH 5.5) was adsorbed for 10 min, followed by a washing step of 10 min. Afterwards, ALG solution was flowed for 6 min to allow ALG adsorption until equilibrium at the crystal surface was reached. After rinsing with 0.1 M sodium acetate buffer/0.15 M NaCl (4 min), the same procedure was followed for CHI deposition. These steps were repeated to generate 5 bilayers. The frequency and dissipation were monitored in real time. The thickness of the film was estimated using the *Voigt* model using the Q-Tools Software (Q-Sense).[47] For the model, solvent viscosity was fixed at 0.001 Pas (water) and the film density at 1050 kg m^{-3} (often assumed to return the lowest calculation error).[48–50] The solvent density was varied by trial and error until the total error, $\chi 2$, was minimized.

Scanning Electronic Microscopy (SEM)

The morphology of the different multilayered films formulations was observed by Scanning Electronic Microscopy (SEM), using a Jeol JSM-6010LV microscope operated at an accelerating voltage of 15 kV. All samples were sputtered with a conductive gold layer, using a sputter coater 108A (Cressington, UK). Three samples were evaluated for each condition.

Atomic Force Microscopy (AFM) Imaging

The multilayered films were imaged using a dimension Icon microscope controlled by NanoScope 9.1 (Bruker, France), operating in peak force tapping (ScanAsyst) mode with quantitative nanomechanical analysis, following established protocols.[51, 52] AFM silicon nitride cantilevers (ScanAsyst-Air, Bruker) with a spring constant of 0.5 N/m, a frequency of 70 kHz, and a radius of the tip of 5 nm were used. The peak-force set-point was adjusted to 3.0 μN and the Poisson's ratio was assumed to be equal to 0.3 for the entire 512×512 pixels (2×2 μm^2) scan of the sample. The line scan rate was 0.4 Hz. The root mean squared roughness (R_{RMS}), average height value (H_{av}), and average elastic modulus (E_{av}) were calculated for each formulation in the wet state. Image analysis was performed using Gwyddion and Nanoscope Analysis 1.5. At least three measurements were performed indifferent specimens.

Water Contact Angle (WCA)

The wettability of the multilayered films was characterized by WCA measurements. Static WCA measurements were performed using the sessile drop method on an OCA15+ goniometer (DataPhysics, Germany) at room temperature. Milli-Q water (6 μL) was dropped onto the PEMs and pictures were taken after water drop stabilization.

Determination of Cross-linking Degree

The cross-linking of CHI/ALG multilayers was evaluated using the Trypan blue method, using a published protocol. [27, 43] Briefly, the test was performed by immersing uncross-linked and cross-linked multilayers in 0.4 % Trypan blue (Invitrogen, USA) diluted 50-fold in sodium acetate buffer overnight at 37° C. The supernatant absorbance was measured at 580 nm in a microplate reader (Sinergy HT, Bio-Tek, USA). The cross-linking degree was calculated as follows:

$$\mathrm{CL}\,(\%)=\frac{(\mathrm{NH_3^+\,non-Xlinked\,solution})-(\mathrm{NH_3^+\,Xlinked\,solution})}{(\mathrm{NH_3^+\,non-Xlinked\,solution})}$$

Where NH_3^+ non-Xlinked and NH_3^+ Xlinked solution are the free charge amines in uncross-linked and in cross-linked multilayers, respectively.

Protein adsorption resistance

The resistance to protein adsorption of modified of the multilayered films with and without cross-linking were evaluated using AlexaFluor488-labeled donkey anti-mouse IgG (Invitrogen, USA). Multilayers with and without cross-linking were incubated in IgG-AF488 for 60 min followed by extensive washing in PBS solution. Samples were immediately observed in a fluorescence microscope (TE300, Nikon, USA). To quantify the differences between ALG/CHI with and without cross-linking as well as the effect of multilayer numbers on the top of the film, a more sensitive protein assay was performed using alkaline phosphatase-conjugated donkey anti-mouse IgG (Jackson Immunoresearch, USA). All multilayers formulations were incubated with 1 μg mL^{-1} of this protein for 30 min, followed by extensive washing in PBS (Gibco, USA) containing 0.05% (v/v) Trinton-X-100 (Sigma, USA). Samples were then immersed in 4-methylumbelliferyl phosphate (25 mg/mL) in diethanolamine buffer for 15 min. Supernatant was collected and the fluorescence was measured on a microplate reader (HTS Plus, Perkin Elmer, USA), using an excitation of 360 nm and emission of 465 nm.

Cell Adhesion to PEMs

Cell culture studies were performed with human umbilical vein endothelial cells (HUVECs, Lonza, USA) during passages 2–6. Cells were cultured in endothelial basal medium (EBM-2; Lonza, Switzerland), supplemented with Endothelial Growth Medium (EGM-2 SingleQuots, Lonza, USA) containing 2 % fetal bovine serum (FBS), 5 ng mL^{-1} epidermal growth, 10 ng mL^{-1} basic fibroblast growth factor, 20 ng mL^{-1} insulin-like growth factor, 0.5 ng mL^{-1} vascular endothelial growth factor, 1 μg mL^{-1} ascorbic acid, 22.5 μg mL^{-1} heparin, 0.2 μg mL^{-1} hydrocortisone, penicillin (200 U/ml), 200 μg mL^{-1} streptomycin, and 0.25 μg mL^{-1} amphotericin B. All substrates (i.e., 96 well plates coated with PEMs and control (TCPS)) were sterilized by exposure to ultraviolet light for 40 min. Cells were seeded at 9000 cells/cm^2 and cultured for 1 day in EBM-2 supplemented with EGM-2 at 37°C in a humidified 5% CO_2 atmosphere. 4,6-diaminidino-2-phenylindole-dilactate (DAPI, Sigma-Aldrich, USA) and Alexa Fluor 488-conjugated phalloidin (Invitrogen, USA) were used to label nuclei and actin cytoskeleton. Briefly at each time point, culture medium was

removed and the samples fixed in 4% (v/v) paraformaldehyde (Electron Microscopy Science, USA) for 1 h, and replaced by PBS. Cells were permeabilized with 0.2% Triton X-100 (Sigma, USA) in PBS for 5 min. Samples were incubated in 30 mg mL^{-1} bovine albumin serum (BSA, Sigma, USA) for 30 min to block non-specific binding. Following PBS washing, DAPI (300 nM) and phalloidin (33 nM) staining was performed for 40 min at RT and protected from light. After extensive washing, samples were visualized in an inverted fluorescence microscope (TE300, Nikon, USA). The images obtained were analyzed using Image J software to determine cell area and density. In addition, cellular tests on native and cross-linked films with or without ALG/CHI multilayers on the top of PEMs were also performed in medium with or without serum.

Cell proliferation was measured using a Click-iT EdU Imaging Kit (Invitrogen, C10340, USA). After 3 h of incubation, half of the medium was removed and 10 mM EdU solution was added to the samples. After 24 h, the samples were washed with PBS, followed by cell fixation with 4% paraformaldehyde for 40 min. After permeabilization, samples were washed with 3% BSA twice and ClickiT reaction cocktail was added, followed by 30 min of incubation and by a washing step. For nucleus staining, Hoechst 33342 solution (30 mM, Fisher Scientific, USA) was added for 30 min, followed by extensive washing with PBS. The samples were visualized using an inverted fluorescence microscope (TE300, Nikon, USA). The images obtained were analyzed using Image J software to determine the percentage of EdU-positive nuclei as a measure of proliferation.

Statistical analyses

The experiments were carried out in triplicate unless otherwise specified. The results were presented as mean ± standard error of mean (SEM). Statistical analysis was performed by one-way ANOVA followed by Tukey pair-wise tests using Graph Pad Prism 5.0 for Windows.

Results and Discussion

LbL assembly of ALG/CHI multilayers

The assembly of 5 bilayers of ALG/CHI multilayered films was monitored *in situ* by QCM-D. Figure 1A shows the buildup of 5 bilayers of ALG/CHI, in terms of variations on normalized resonance frequency ($\Delta f_7/7$) and dissipation (ΔD_7) of the seventh overtone (35 MHz). Before the deposition of marine polysaccharides, PEI was flushed into the system, which confers a positive charge, as well as, an homogeneous deposition of PEMs.[53] As expected, the normalized frequency decreases upon each flushing of polyelectrolyte solution, reflecting the increase of mass over the gold sensor (including water), and the deposition of polymer on the surface of the crystal. On the other hand, the ΔD_7 mirrors the behavior of Δf_7, and a decrease is observed revealing that the film is not rigid and exhibits the typical viscoelastic behavior, which is characteristic of macromolecular systems. In addition, such variation indicates a shift toward a film with a higher viscous component and a great ability to adsorb water.[37, 48] During the washing steps, the change of both $\Delta f_7/7$ and ΔD_7 are relatively small, indicating a strong association of the layers on the surface of the quartz crystal, and a weak desorption. The ladder trace of $\Delta f_7/7$ decrease and the trace of

ΔD_7 increase, indicating the alternative adsorption of ALG or CHI molecules onto the substrate. The decrease in $\Delta f_n/n$ for the other overtones is different, which indicates that the adsorbed layer does not obey the Sauerbey law, as it was previously reported for these multilayers (Figure 2B).[34] Thus, the thickness of the film was estimated modeling the frequency and dissipation data, using the Voigt model instead of the Sauerbrey model.[47] For viscoelastic materials, the adsorbed mass does not fully couple to the oscillation of the crystal and dampens the oscillation, making the use of the *Voigt* model more appropriate. [34, 47] The film thickness increased linearly with the deposited layers, as previously reported [27, 34, 44, 54]. A thickness of ~80 nm was estimated for the final 5 bilayers. The thickness of the film is related to the water-uptake of each polyelectrolyte, the charge matching between the polyelectrolyte pairs and the affinity of polyelectrolytes for each other.[32]

Physicochemical characterization

The surface properties of the multilayers such as morphology, topography and wettability influence protein adsorption and cell behavior. As previously reported, using ALG and CHI as polyelectrolytes lead to robust and compliant multilayers.[34, 44, 46] In the present work, the multilayered films were cross-linked with genipin (G, 3.5 mg mL^{-1}, cross-linking degree ≈65%) to improve their stability at all pH values, biodegradability, hydration, and mechanical strength. The morphology of different multilayer formulations was evaluated by SEM (Figure 2A and S1). The results reveal a similar surface topography among different formulations and an increase in film's homogeneity as the number of bilayers increases. In order to have a better understanding of films topography at a smaller scale, AFM analysis was also performed. All formulations exhibit a rough surface, represented by polymer aggregates, usually called "islets" (Figure 2B – 2D). It is also important to point out that one should be aware that the surface may not be fully coated, as suggested in previous works of Richert and coworkers.[55] Upon chemical cross-linking, the mean squared roughness (R_{RMS}) and average height value (H_{av}) increase due to the formation of a semi-interpenetrating network where ALG chains remain entrapped the cross-linked CHI chains. [44] It should also be pointed out that upon addition of multilayers on the top of the cross-linked films the roughness slightly increases.

The cross-linking of multilayers with genipin gives rise to semi-interpenetrating networks, since genipin only interacts with polyelectrolyte containing free amine groups (i.e. the amine groups that are not involved in the electrostatic interactions) (Figure 3A). Using genipin, both color and fluorescence are generated upon its efficient reaction with primary amine groups and oxygen-radical induced polymerization.[28, 56] The Trypan blue assay was performed to determine the cross-linking degree of the CHI within the multilayers.[57] The cross-linking degree could be varied from 0 % to 65 % by simple adjustment of the cross-linker concentration.

AFM experiments were also performed to assess the mechanical properties of the multilayered films (Fig. 3C). The elastic modulus (E_{av}) increases from 199.2 ± 46.5 MPa to 842.2 ± 79.5 MPa upon cross-linking. The results confirm an increase in stiffness upon increasing the cross-linker concentration which corroborated the results obtained in Trypan

blue assay (Figure S2A). In addition, the results confirm an increase in stiffness upon cross-linking and/or by adding bilayers on the top of the film which can be explained by an increase on film's homogeneity and thickness, which corroborated the AFM and QCM-D results.

In contrast to EDC/s-NHS-based cross-linking, genipin reaction is not a "zero length" reaction, since additional monomers and further dimerization are introduced within the film, altering the chemistry of the surface. It has been reported that genipin acts through nucleophilic attack of CHI amine groups, establishing a secondary amide linkage.[28, 56] Subsequent steps involve radical-induced polymerization that creates genipin heterocyclic derivatives, which are richer in hydrophilic groups such as amine, amides and hydroxyl groups.[28, 56] The wetting behavior of the multilayered films was evaluated by water contact angle (WCA) measurements. Figure 3D shows that WCA decreases upon cross-linking, decreasing gradually with increases in the cross-linker concentration (Figure S2B). This finding is consistent with earlier studies where a consistent decrease of WCA was found with increasing cross-linker concentrations.[28, 39] This decrease has been previously explained by the denser polyelectrolyte connections and increase of cross-linker conjugates within the films.[44] In addition, upon the adsorption of another bilayer on the top of uncross-linked or cross-linked films, the WCA increases due to changes on the surface chemistry. Upon deposition of ALG/CHI bilayers on the top of the cross-linked films (G +1/G+2) the chemistry of the surface is changed, masking the hydrophilic character of the cross-linker derivatives.

Protein adsorption resistance

The resistance to IgG adsorption of these multilayers was evaluated by measuring the adsorption of labeled IgG onto these monolayers (Figure 4A). Upon cross-linking with genipin, adsorption of IgG-AF488 substantially decreased. In order to quantify the effects of cross-linking on protein adsorption, an assay based on donkey anti-mouse IgG antibody conjugated to alkaline phosphatase was performed (Figure 4B). In this assay the same trend was observed, and a decrease on substrate reaction occurs following chemical cross-linking. However, this behavior is reversed with the addition of another bilayer of ALG and CHI on the top of cross-linked films prior to exposure to IgG. The addition of another bilayer effectively acts as a physical barrier for the underlying cross-linked films, leading to 2-fold increase in the fluorescence intensity when compared to the cross-linked films. These results were further confirmed by WCA, where a decrease in the hydrophilicity of cross-linked multilayers is observed upon the addition of a multilayer on top of cross-linked films (Figure 3D). To establish the general protein adsorption resistant properties of these films however, additional proteins must be evaluated.

Cell Adhesion to ALG/CHI Films

Multilayers based on polysaccharides are resistant to cell adhesion due to high hydration and low stiffness.[27–29] However, these multilayers can also be used to control cellular behavior upon tailoring the mechanical properties (matrix stiffness, elasticity and viscosity), which influence how cells spread, migrate, proliferate, differentiate, and organize key intracellular structures.[44, 58] Herein, using different genipin concentrations ranging from

0–5 mg mL^{-1}, an increase in cell number and spread area and a decrease in cell circularity occur with increases in cross-linker concentration (Figure 5). In addition, cell density increases linearly with cross-linking degree (r^2= 0.98) (Figure 5C), and the cell morphology, number, area, and proliferation are in the same range as values for cells adhering to TCPS (Figure S3). Similar behavior is observed for cell density, spread area and circularity plotted as a function of E_{av} (Figure 6). However, cell density was not linearly increasing with E_{av}, because certain cross-linker concentrations led to an increase of cross-linking degree and to minor differences on E_{av}. These results corroborated previous reports, where CHI/ALG multilayers upon cross-linking with genipin presented a decrease in water-uptake ability, decrease in the viscous component of the film, increase in stiffness and enhancements in cell adherence, spreading and proliferation.[43, 59] Similar behavior has also been reported for other multilayers [36, 60, 61], and for a large variety of cells, including endothelial cells, which prefer stiffer substrate (i.e., less gel-like substrates) for attachment and spreading.[53]

We also tailored the cell adhesive properties of the multilayers by the adsorption or immobilization of ECM proteins (e.g. FN and LM). Using this approach, cell number and spread area increase, whereas the circularity decreases, with adsorption or immobilization of these ECM components (Figure 7). Similar results have been reported for multilayered films containing FN [62, 63] or LM [64, 65]. High cell adhesive and proliferation activities were observed for FN compared to LM. These differences may arise from the higher molecular weight of LM compared to FN which may affect its conformation and orientation upon adsorption or immobilization onto the multilayers. In addition, larger proteins bind more strongly and can even repel pre-adsorbed proteins during post-adsorption spreading.[66]

Our data demonstrate that both cross-linking and ECM immobilization modulate cell adhesion. We next combined films cross-linked with two different genipin concentrations (3.5 and 5 mg mL^{-1}) with ECM proteins by adsorption or immobilization. This analysis reveals a modest impact of protein adsorption or immobilization on cell behavior when compared with the uncross-linked film (Figure S4 and S5). Similar results have been reported for poly(L-lysine)/poly(L-glutamic acid) (PLL/PGA) multilayers upon cross-linking and grafting with arginine-glycine-aspartic acid (RGD).[67] Covalent cross-linking enhances endothelial cell adhesion and allows high cellular coverage without the pre-adsorption or immobilization of ECM proteins. However, the cell adhesion was hindered upon deposition of additional bilayers of polyelectrolytes on the top of cross-linked films (3.5 mg mL^{-1}, cross-linking degree ≈ 60.5 %) (Figure 8). Finally, EdU labeling demonstrates a decrease in endothelial cell proliferation upon addition of ALG/CHI bilayers on top of cross-linked films. However, upon adsorption or immobilization of ECM proteins, cell proliferation was enhanced. The positive effect of ECM proteins on HUVECs proliferation has been reported for PEMs.[31, 63, 68]

As the number of bilayerson the top of cross -linked films increase, the resistance to cell adhesion was more pronounced (Figure S6). However, upon adsorption or immobilization of ECM proteins, the cell adhesive and proliferation properties of PEMs were recovered. We performed a similar study with uncross-linked films, and additional layers were deposited on the top of the film, which further decreased the cell spread area and cell density (Figure 9 and S7). Notably, Richert *et al.* demonstrated that the number of layers influence cellular

responses, because it led to an increase of thickness and higher hydration rates.[69–71] EdU labeling indicated a decrease in cell proliferation upon the adsorption of bilayers on the top of cross-linked films and no differences for native films. These results highlight the key role of surface chemistry on cell proliferation.

To evaluate the contribution of the adsorption of serum proteins on cell adhesion on multilayered films, adhesion experiments were performed in serum-free media (Figure 10 and S8). For cross-linked films, endothelial cells adhered and spread on the surface even in serum-free media conditions, indicating that the adhesion was not primarily mediated by the proteins present in serum but by the mechanical and chemical cues on the substrate and/or proteins secreted by the cells. For native films the same behavior was observed, validating results where cell adhesion and proliferation were achieved upon chemical cross-linking or ECM proteins adsorption/immobilization.

Conclusion

We present a strategy to tune the cell adhesive properties of multilayers based on ALG and CHI with and without cross-linking and/or coating with ECM proteins. Chemical cross-linking of multilayers improved mechanical properties of the coatings but also elicited changes in surface chemistry that alter the adhesion of human umbilical vein endothelial cells. Addition of CHI/ALG multilayers on top of cross-linked films decreased endothelial cell adhesion, spreading, and proliferation to similar levels as uncross-linked films. Our findings highlight the key role of surface chemistry in cell-multilayer film interactions, and these engineered nanocoatings represent a tunable model of cell adhesive and non-adhesive multilayered films.

Supplementary Material

Refer to Web version on PubMed Central for supplementary material.

Acknowledgments

The authors acknowledge the financial support by the Luso-American Foundation and the USA National Institutes of Health (R01 AR062920). Joana M. Silva would also like to acknowledge the Portuguese Foundation for Science and Technology(FCT) for her PhD grant.

References

1. Ariga K, Hill JP, Ji Q. Layer-by-layer assembly as a versatile bottom-up nanofabrication technique for exploratory research and realistic application. Physical Chemistry Chemical Physics. 2007; 9:2319–40. [PubMed: 17492095]
2. Boudou T, Crouzier T, Ren K, Blin G, Picart C. Multiple Functionalities of Polyelectrolyte Multilayer Films: New Biomedical Applications. Advanced Materials. 2010; 22:441–67. [PubMed: 20217734]
3. De Villiers MM, Otto DP, Strydom SJ, Lvov YM. Introduction to nanocoatings produced by layer-by-layer (LbL) self-assembly. Adv Drug Delivery Rev. 2011; 63:701–15.
4. Decher, G. Multilayer thin films. 2. Wiley; Weinheim: 2012. Layer-by-layer assembly (putting molecules to work); p. 1-21.
5. Detzel CJ, Larkin AL, Rajagopalan P. Polyelectrolyte multilayers in tissue engineering. Tissue Engineering Part B: Reviews. 2011; 17:101–13. [PubMed: 21210759]

6. Hammond PT. Engineering materials layer-by-layer: Challenges and opportunities in multilayer assembly. AIChE Journal. 2011; 57:2928–40.
7. Tang Z, Wang Y, Podsiadlo P, Kotov NA. Biomedical Applications of Layer-by-Layer Assembly: From Biomimetics to Tissue Engineering. Advanced Materials. 2006; 18:3203–24.
8. Lvov Y, Decher G, Moehwald H. Assembly, structural characterization, and thermal behavior of layer-by-layer deposited ultrathin films of poly (vinyl sulfate) and poly (allylamine). Langmuir. 1993; 9:481–6.
9. Iler R. Multilayers of colloidal particles. Journal of colloid and interface science. 1966; 21:569–94.
10. Lim F, Sun AM. Microencapsulated islets as bioartificial endocrine pancreas. science. 1980; 210:908–10. [PubMed: 6776628]
11. Hammond PT. Form and function in multilayer assembly: new applications at the nanoscale. Advanced Materials. 2004; 16:1271–93.
12. Hammond PT. Building biomedical materials layer-by-layer. Materials Today. 2012; 15:196–206.
13. Borges J, Mano JF. Molecular interactions driving the layer-by-layer assembly of multilayers. Chemical reviews. 2014; 114:8883–942. [PubMed: 25138984]
14. Aggarwal N, Altgärde N, Svedhem S, Michanetzis G, Missirlis Y, Groth T. Tuning Cell Adhesion and Growth on Biomimetic Polyelectrolyte Multilayers by Variation of pH During Layer-by-Layer Assembly. Macromolecular bioscience. 2013; 13:1327–38. [PubMed: 23840005]
15. Salloum DS, Olenych SG, Keller TC, Schlenoff JB. Vascular smooth muscle cells on polyelectrolyte multilayers: hydrophobicity-directed adhesion and growth. Biomacromolecules. 2005; 6:161–7. [PubMed: 15638516]
16. Ghostine RA, Markarian MZ, Schlenoff JB. Asymmetric growth in polyelectrolyte multilayers. Journal of the American Chemical Society. 2013; 135:7636–46. [PubMed: 23672490]
17. Vidyasagar A, Sung C, Losensky K, Lutkenhaus JL. pH-dependent thermal transitions in hydrated layer-by-layer assemblies containing weak polyelectrolytes. Macromolecules. 2012; 45:9169–76.
18. Burke SE, Barrett CJ. Swelling behavior of hyaluronic acid/polyallylamine hydrochloride multilayer films. Biomacromolecules. 2005; 6:1419–28. [PubMed: 15877361]
19. Jang Y, Seo J, Akgun B, Satija S, Char K. Molecular weight dependence on the disintegration of spin-assisted weak polyelectrolyte multilayer films. Macromolecules. 2013; 46:4580–8.
20. Hammond PT. Recent explorations in electrostatic multilayer thin film assembly. Current Opinion in Colloid & Interface Science. 1999; 4:430–42.
21. Malafaya PB, Silva GA, Reis RL. Natural–origin polymers as carriers and scaffolds for biomolecules and cell delivery in tissue engineering applications. Advanced Drug Delivery Reviews. 2007; 59:207–33. [PubMed: 17482309]
22. Cascone M, Barbani NP, Giusti CC, Ciardelli G, Lazzeri L. Bioartificial polymeric materials based on polysaccharides. Journal of Biomaterials Science, Polymer Edition. 2001; 12:267–81. [PubMed: 11484936]
23. Mano JF, Silva GA, Azevedo HS, Malafaya PB, Sousa RA, Silva SS, Boesel LF, Oliveira JM, Santos TC, Marques AP, Neves NM, Reis RL. Natural origin biodegradable systems in tissue engineering and regenerative medicine: present status and some moving trends. Journal of the Royal Society Interface. 2007; 4:999–1030.
24. Brown SH, Pummill PE. Recombinant production of hyaluronic acid. Current pharmaceutical biotechnology. 2008; 9:239–41. [PubMed: 18691082]
25. Etienne O, Schneider A, Taddei C, Richert L, Schaaf P, Voegel J-C, Egles C, Picart C. Degradability of polysaccharides multilayer films in the oral environment: an in vitro and in vivo study. Biomacromolecules. 2005; 6:726–33. [PubMed: 15762636]
26. Picart C, Schneider A, Etienne O, Mutterer J, Schaaf P, Egles C, Jessel N, Voegel J-C. Controlled degradability of polysaccharide multilayer films in vitro and in vivo. Advanced Functional Materials. 2005; 15:1771–80.
27. Silva JM, Caridade SG, Costa RR, Alves NM, Groth T, Picart C, Reis RL, Mano JF. pH Responsiveness of Multilayered Films and Membranes Made of Polysaccharides. Langmuir. 2015; 31:11318–28. [PubMed: 26421873]

28. Gao L, Gan H, Meng Z, Gu R, Wu Z, Zhang L, Zhu X, Sun W, Li J, Zheng Y, Dou G. Effects of genipin cross-linking of chitosan hydrogels on cellular adhesion and viability. Colloids and Surfaces B: Biointerfaces. 2014; 117:398–405. [PubMed: 24675278]
29. Gaudière F, Morin-Grognet S, Bidault L, Lembré P, Pauthe E, Vannier J-P, Atmani H, Ladam G, Labat Ba. Genipin-Cross-Linked Layer-by-Layer Assemblies: Biocompatible Microenvironments To Direct Bone Cell Fate. Biomacromolecules. 2014; 15:1602–11. [PubMed: 24666097]
30. Silva JM, Reis RL, Mano JF. Biomimetic Extracellular Environment Based on Natural Origin Polyelectrolyte Multilayers. Small. 2016; 12:4308–42. [PubMed: 27435905]
31. Li G, Yang P, Liao Y, Huang N. Tailoring of the titanium surface by immobilization of heparin/fibronectin complexes for improving blood compatibility and endothelialization: an in vitro study. Biomacromolecules. 2011; 12:1155–68. [PubMed: 21332186]
32. Gribova V, Auzely-Velty R, Picart C. Polyelectrolyte Multilayer Assemblies on Materials Surfaces: From Cell Adhesion to Tissue Engineering. Chemistry of Materials. 2011; 24:854–69.
33. Boddohi S, Killingsworth CE, Kipper MJ. Polyelectrolyte multilayer assembly as a function of pH and ionic strength using the polysaccharides chitosan and heparin. Biomacromolecules. 2008; 9:2021–8. [PubMed: 18564872]
34. Alves NM, Picart C, Mano JF. Self Assembling and Crosslinking of Polyelectrolyte Multilayer Films of Chitosan and Alginate Studied by QCM and IR Spectroscopy. Macromolecular Bioscience. 2009; 9:776–85. [PubMed: 19340816]
35. Larkin AL, Davis RM, Rajagopalan P. Biocompatible, detachable, and free-standing polyelectrolyte multilayer films. Biomacromolecules. 2010; 11:2788–96. [PubMed: 20815399]
36. Richert L, Boulmedais F, Lavalle P, Mutterer J, Ferreux E, Decher G, Schaaf P, Voegel J-C, Picart C. Improvement of stability and cell adhesion properties of polyelectrolyte multilayer films by chemical cross-linking. Biomacromolecules. 2004; 5:284–94. [PubMed: 15002986]
37. Picart C, Lavalle P, Hubert P, Cuisinier F, Decher G, Schaaf P, Voegel J-C. Buildup mechanism for poly (L-lysine)/hyaluronic acid films onto a solid surface. Langmuir. 2001; 17:7414–24.
38. Ren K, Crouzier T, Roy C, Picart C. Polyelectrolyte multilayer films of controlled stiffness modulate myoblast cells differentiation. Advanced Functional Materials. 2008; 18:1378. [PubMed: 18841249]
39. Hillberg AL, Holmes CA, Tabrizian M. Effect of genipin cross-linking on the cellular adhesion properties of layer-by-layer assembled polyelectrolyte films. Biomaterials. 2009; 30:4463–70. [PubMed: 19520425]
40. Cui L, Jia J, Guo Y, Liu Y, Zhu P. Preparation and characterization of IPN hydrogels composed of chitosan and gelatin cross-linked by genipin. Carbohydrate Polymers. 2014; 99:31–8. [PubMed: 24274476]
41. Mekhail M, Jahan K, Tabrizian M. Genipin-crosslinked chitosan/poly-l-lysine gels promote fibroblast adhesion and proliferation. Carbohydrate Polymers. 2014; 108:91–8. [PubMed: 24751251]
42. Chaubaroux C, Vrana E, Debry C, Schaaf P, Senger B, Voegel J-C, Haikel Y, Ringwald C, Hemmerlé J, Lavalle P, Boulmedais F. Collagen-Based Fibrillar Multilayer Films Cross-Linked by a Natural Agent. Biomacromolecules. 2012; 13:2128–35. [PubMed: 22662909]
43. Silva JM, Duarte ARC, Caridade SG, Picart C, Reis RL, Mano JF. Tailored Freestanding Multilayered Membranes Based on Chitosan and Alginate. Biomacromolecules. 2014; 15:3817–26. [PubMed: 25244323]
44. Silva JM, Caridade SG, Oliveira NM, Reis RL, Mano JF. Chitosan–alginate multilayered films with gradients of physicochemical cues. Journal of Materials Chemistry B. 2015; 3:4555–68.
45. Engler A, Bacakova L, Newman C, Hategan A, Griffin M, Discher D. Substrate compliance versus ligand density in cell on gel responses. Biophysical journal. 2004; 86:617–28. [PubMed: 14695306]
46. Caridade SG, Monge C, Gilde F, Boudou T, Mano JF, Picart C. Free-Standing Polyelectrolyte Membranes Made of Chitosan and Alginate. Biomacromolecules. 2013; 14:1653–60. [PubMed: 23590116]

47. Voinova MV, Rodahl M, Jonson M, Kasemo B. Viscoelastic Acoustic Response of Layered Polymer Films at Fluid-Solid Interfaces: Continuum Mechanics Approach. Phys Scr. 1999; 59:391–6.

48. Costa RR, Custódio CA, Arias FJ, Rodríguez-Cabello JC, Mano JF. Layer-by-Layer Assembly of Chitosan and Recombinant Biopolymers into Biomimetic Coatings with Multiple Stimuli-Responsive Properties. Small. 2011; 7:2640–9. [PubMed: 21809443]

49. Dutta AK, Belfort G. Adsorbed gels versus brushes: viscoelastic differences. Langmuir. 2007; 23:3088–94. [PubMed: 17286418]

50. Weber N, Pesnell A, Bolikal D, Zeltinger J, Kohn J. Viscoelastic properties of fibrinogen adsorbed to the surface of biomaterials used in blood-contacting medical devices. Langmuir. 2007; 23:3298–304. [PubMed: 17291015]

51. Alsteens D, Dupres V, Yunus S, Latgé J-P, Heinisch J Jr, Dufrêne YF. High-resolution imaging of chemical and biological sites on living cells using peak force tapping atomic force microscopy. Langmuir. 2012; 28:16738–44. [PubMed: 23198968]

52. Trtik P, Kaufmann J, Volz U. On the use of peak-force tapping atomic force microscopy for quantification of the local elastic modulus in hardened cement paste. Cement and concrete research. 2012; 42:215–21.

53. Boura C, Menu P, Payan E, Picart C, Voegel J, Muller S, Stoltz J. Endothelial cells grown on thin polyelectrolyte mutlilayered films: an evaluation of a new versatile surface modification. Biomaterials. 2003; 24:3521–30. [PubMed: 12809781]

54. Martins GV, Merino EG, Mano JF, Alves NM. Crosslink Effect and Albumin Adsorption onto Chitosan/Alginate Multilayered Systems: An in situ QCM-D Study. Macromolecular Bioscience. 2010; 10:1444–55. [PubMed: 21125694]

55. Richert L, Lavalle P, Payan E, Shu XZ, Prestwich GD, Stoltz J-F, Schaaf P, Voegel J-C, Picart C. Layer by Layer Buildup of Polysaccharide Films: Physical Chemistry and Cellular Adhesion Aspects. Langmuir. 2004; 20:448–58. [PubMed: 15743090]

56. Chen H, Ouyang W, Lawuyi B, Martoni C, Prakash S. Reaction of chitosan with genipin and its fluorogenic attributes for potential microcapsule membrane characterization. Journal of Biomedical Materials Research Part A. 2005; 75A:917–27.

57. Shen W-C, Yang D, Ryser HJP. Colorimetric determination of microgram quantities of polylysine by trypan blue precipitation. Analytical Biochemistry. 1984; 142:521–4. [PubMed: 6549372]

58. Rehfeldt F, Engler AJ, Eckhardt A, Ahmed F, Discher DE. Cell responses to the mechanochemical microenvironment—implications for regenerative medicine and drug delivery. Adv Drug Delivery Rev. 2007; 59:1329–39.

59. Silva JM, Duarte ARC, Custódio CA, Sher P, Neto AI, Pinho A, Fonseca J, Reis RL, Mano JF. Nanostructured hollow tubes based on chitosan and alginate multilayers. Advanced healthcare materials. 2014; 3:433–40. [PubMed: 23983205]

60. Richert L, Schneider A, Vautier D, Vodouhe C, Jessel N, Payan E, Schaaf P, Voegel J-C, Picart C. Imaging cell interactions with native and crosslinked polyelectrolyte multilayers. Cell Biochem Biophys. 2006; 44:273–85. [PubMed: 16456228]

61. Schneider A, Francius G, Obeid R, Schwinté P, Hemmerlé J, Frisch B, Schaaf P, Voegel J-C, Senger B, Picart C. Polyelectrolyte multilayers with a tunable Young's modulus: influence of film stiffness on cell adhesion. Langmuir. 2006; 22:1193–200. [PubMed: 16430283]

62. Wittmer CR, Phelps JA, Lepus CM, Saltzman WM, Harding MJ, Van Tassel PR. Multilayer nanofilms as substrates for hepatocellular applications. Biomaterials. 2008; 29:4082–90. [PubMed: 18653230]

63. Olenych SG, Moussallem MD, Salloum DS, Schlenoff JB, Keller TC. Fibronectin and cell attachment to cell and protein resistant polyelectrolyte surfaces. Biomacromolecules. 2005; 6:3252–8. [PubMed: 16283753]

64. Giamblanco N, Martines E, Marletta G. Laminin adsorption on nanostructures: switching the molecular orientation by local curvature changes. Langmuir. 2013; 29:8335–42. [PubMed: 23742648]

65. He L, Tang S, Prabhakaran MP, Liao S, Tian L, Zhang Y, Xue W, Ramakrishna S. Surface Modification of PLLA Nano-scaffolds with Laminin Multilayer by LbL Assembly for Enhancing Neurite Outgrowth. Macromolecular bioscience. 2013; 13:1601–9. [PubMed: 24038950]

66. Borges J, Campiña JM, Silva AF. Probing the Contribution of Different Intermolecular Forces to the Adsorption of Spheroproteins onto Hydrophilic Surfaces. The Journal of Physical Chemistry B. 2013; 117:16565–76. [PubMed: 24308321]

67. Gribova V, Gauthier-Rouvière C, Albigès-Rizo C, Auzely-Velty R, Picart C. Effect of RGD functionalization and stiffness modulation of polyelectrolyte multilayer films on muscle cell differentiation. Acta biomaterialia. 2013; 9:6468–80. [PubMed: 23261924]

68. Wittmer CR, Phelps JA, Saltzman WM, Van Tassel PR. Fibronectin terminated multilayer films: protein adsorption and cell attachment studies. Biomaterials. 2007; 28:851–60. [PubMed: 17056106]

69. Tryoen-Tóth P, Vautier D, Haikel Y, Voegel JC, Schaaf P, Chluba J, Ogier J. Viability, adhesion, and bone phenotype of osteoblast-like cells on polyelectrolyte multilayer films. Journal of Biomedical Materials Research. 2002; 60:657–67. [PubMed: 11948525]

70. Schneider A, Richert L, Francius G, Voegel J-C, Picart C. Elasticity, biodegradability and cell adhesive properties of chitosan/hyaluronan multilayer films. Biomedical Materials. 2007; 2:S45. [PubMed: 18458419]

71. Dubas ST, Schlenoff JB. Polyelectrolyte multilayers containing a weak polyacid: construction and deconstruction. Macromolecules. 2001; 34:3736–40.

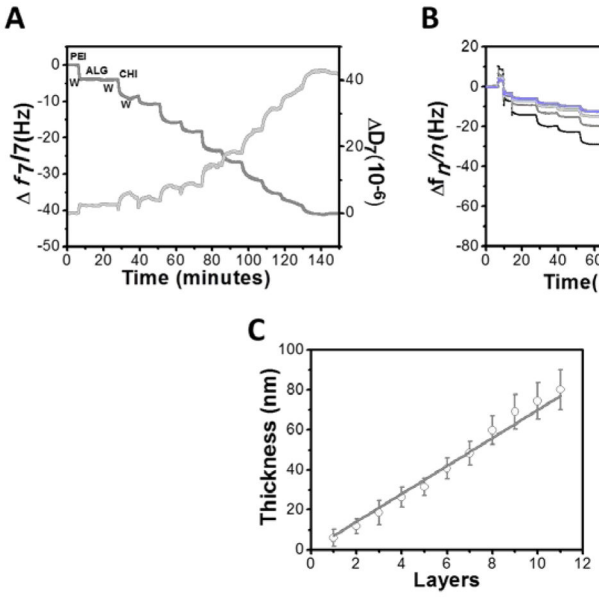

Figure 1.

Monitoring the buildup of five bilayers of ALG/CHI on gold modified initially modified with PEI: (A) Normalized resonance frequency ($\Delta f_7/7$) and dissipation shift (ΔD_7) obtained at 35 MHz; (B) Normalized resonance frequency shift for four overtones (n= 5,7,9,11); (C) Cumulative thickness evolution of polymeric film as a function of the number of deposited layers. Linear fitting matches well with the cumulative thickness variation ($r^2 = 0.99$).

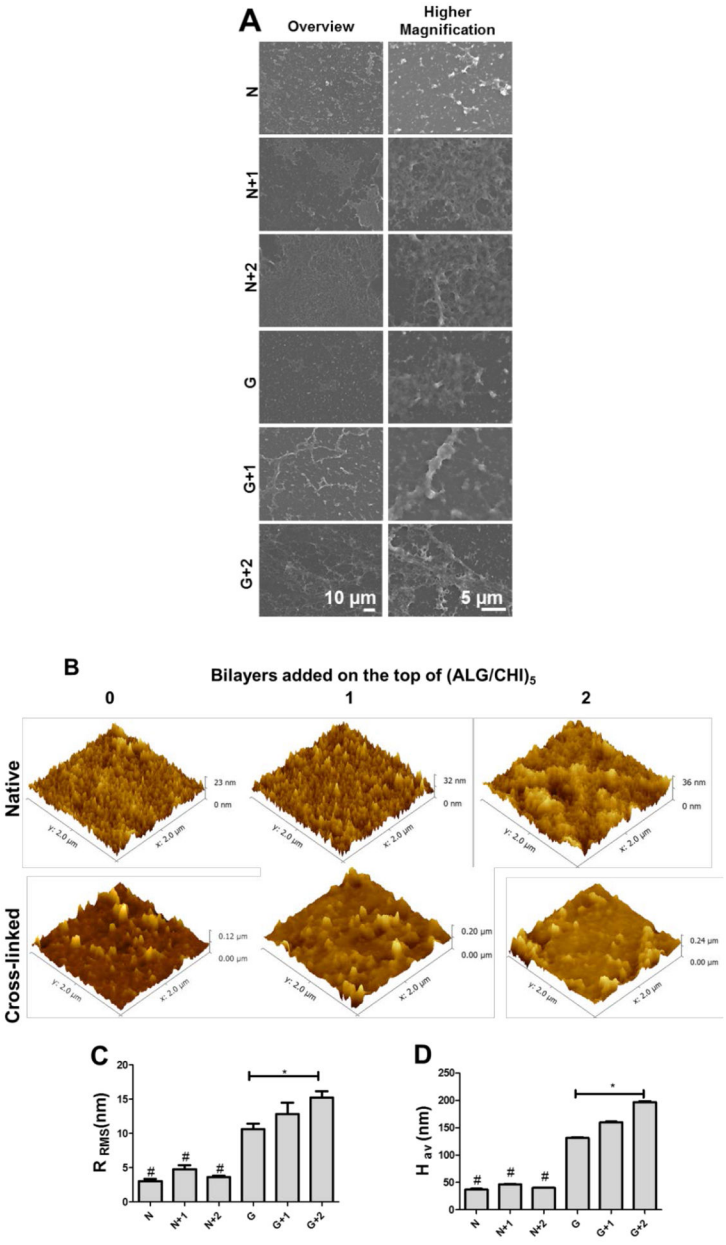

Figure 2.

(A) SEM micrographs of $(ALG/CHI)_5$ multilayers without (N) or with cross-linking (G), as well as with additional bilayers (1 or 2) on the top of the films. (B) AFM images (2×2 μm^2) of $(ALG/CHI)_5$ multilayered films without and with cross-linking upon the addition of bilayers on the top. (C) Root mean squared roughness (R_{RMS}) and (D) Average height value (H_{av}) for the different formulations. Statistical analysis was performed, and data was considered statistically different for p values < 0.05 (*). (#) denotes significant differences when compared to all the native films.

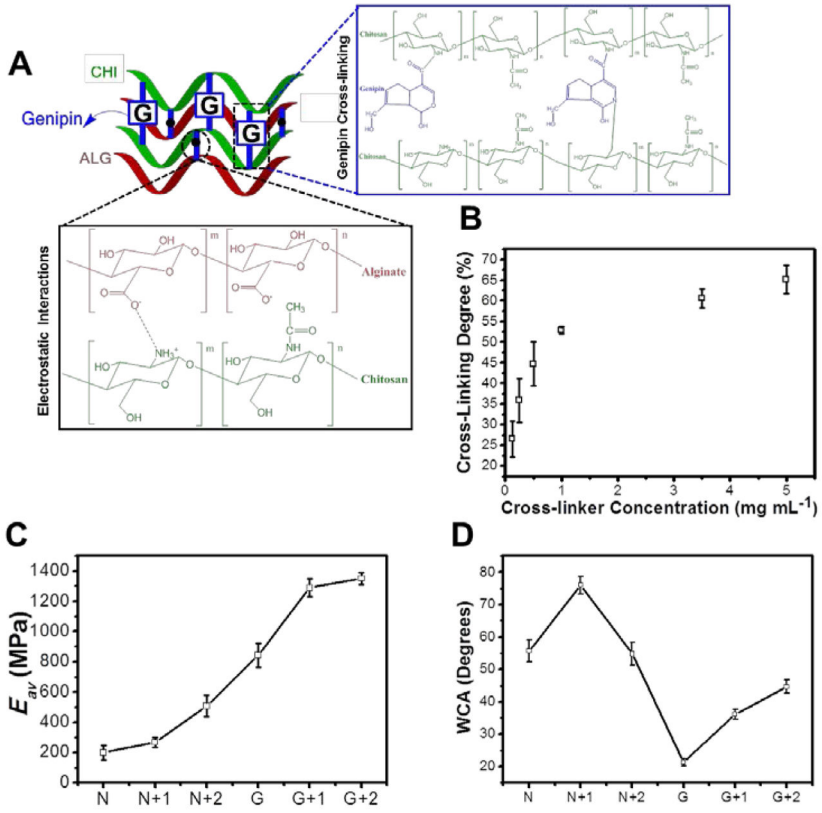

Figure 3.

(A) Schematic representation showing the multilayered rearrangements within the film, namely its electrostatic interactions and genipin cross-linking. (B) Cross-linking degree of ALG/CHI at different genipin concentrations; (C) Elastic modulus (E_{av}) upon cross-linking and/or deposition of bilayers on the top of the films using AFM indentation (D) Water contact angle (WCA) upon cross-linking and/or deposition of bilayers on the top of the films.

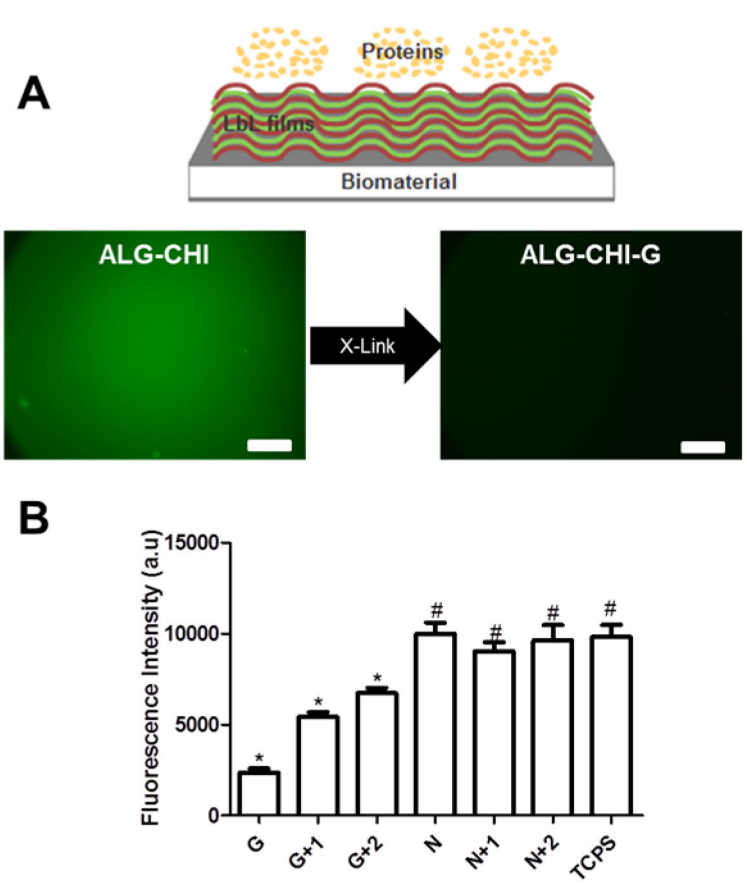

Figure 4.

Non-fouling properties of ALG/CHI films. (A) Donkey anti-mouse IgG AF488 fluorescence assay in multilayers with (G) and without cross-linking (N). The scale bar is 250 μm. The inset image is a schematic representation of non-fouling PEMs. (B) Enzymatic assay for IgG adsorption onto PEMs. Statistical analysis was performed, and data was considered statistically different for p values < 0.05. (*) denotes significant differences when compared to all PEMs formulations. (#) denotes significant differences relative to cross-linked multilayers.

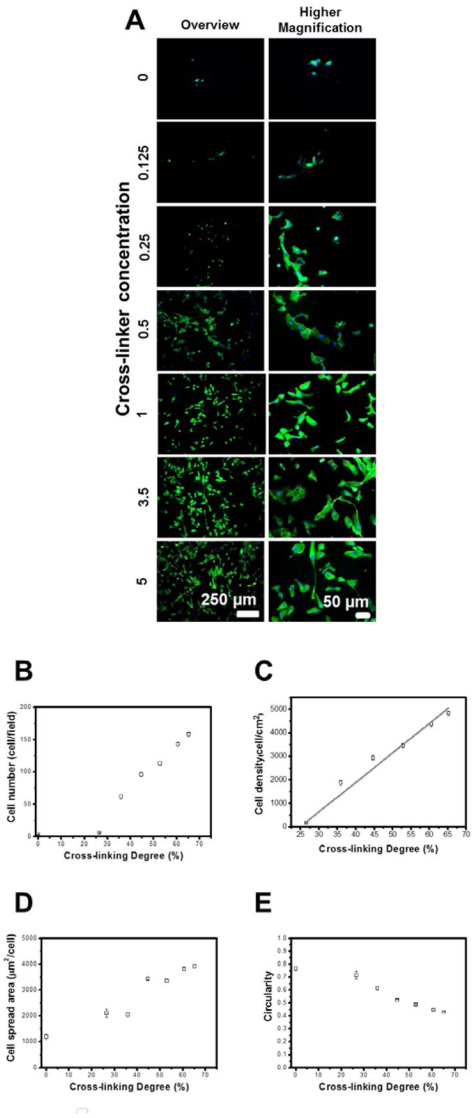

Figure 5.

(A) DAPI-phalloidin fluorescence assay at 1 day of HUVECs culture in multilayers with different cross-linking degrees. Cells nuclei were stained blue by DAPI and F-actin filaments in green by phalloidin. (B) Cell number per field, (C) Cell density and (D) Cell spread area, and (E) Cell circularity as a function of cross-linking degree. Linear fitting matches well with the cell density variation as a function of cross-linking degree ($r^2 = 0.98$). Statistical analysis was performed, and data was considered statistically different for p values < 0.05 (*). (#) denotes significant differences when compared to all PEMs formulations.

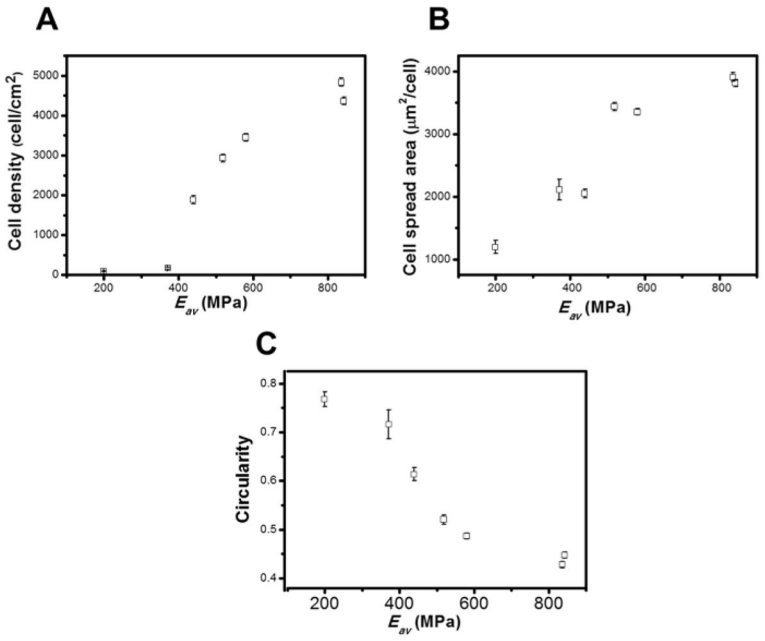

Figure 6.

Cell number per field, (C) Cell density and (D) Cell spread area, and (E) Cell circularity as a function of Elastic modulus (E_{av}).

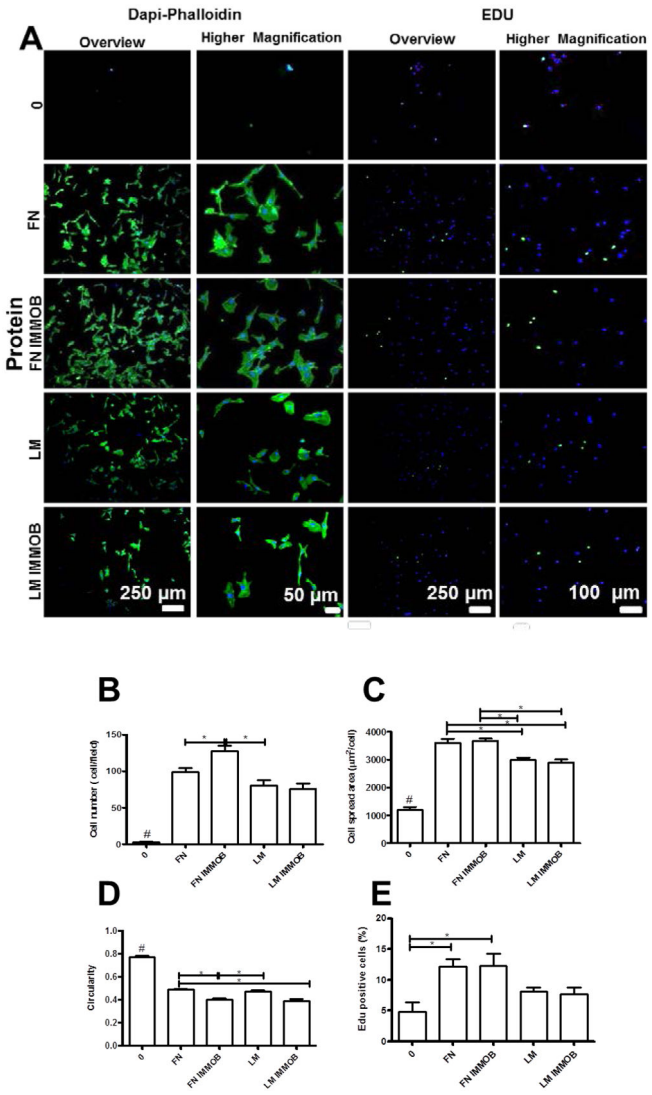

Figure 7.

(A) DAPI/phalloidin staining and representative images of EDU assay for HUVECs adhered on native films with and without adsorbed or immobilized proteins (IMMOB). Quantification of (B) Cell number per field, (C) Cell spread area, and (D) Cell circularity. (E) Percentage of proliferating cells measured by the EDU assay. Statistical analysis was performed, and data was considered statistically different for p values < 0.05 (*). (#) denotes significant differences when compared to all PEMs formulations.

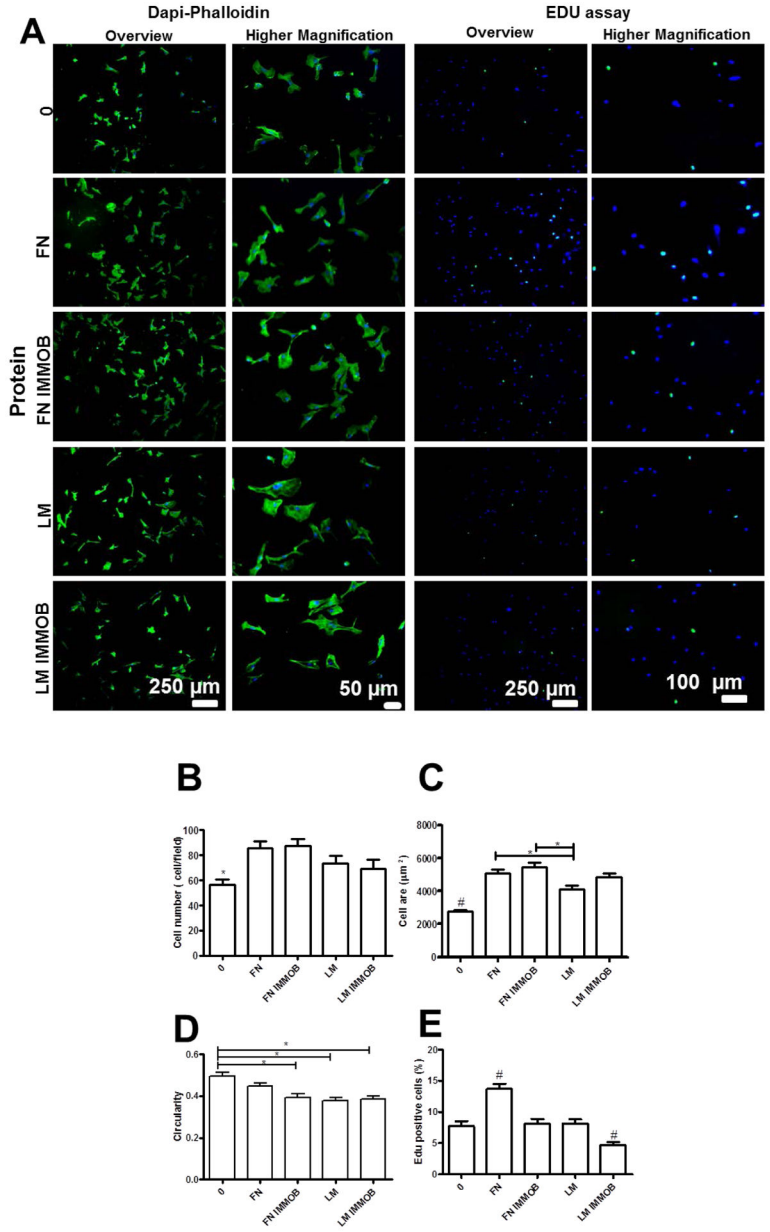

Figure 8.

(A) DAPI/phalloidin staining and representative images of EDU assay for HUVECs adhered on cross-linked films with a bilayer of ALG/CHI on the top in the presence or absence of adsorbed or immobilized proteins (IMMOB). Quantification of (B) Cell number per field, (C) Cell spread area, and (D) Cell circularity. (E) Percentage of proliferating cells measured by the EDU assay. Statistical analysis was performed, and data was considered statistically different for p values < 0.05 (*). (#) denotes significant differences when compared to all PEMs formulations.

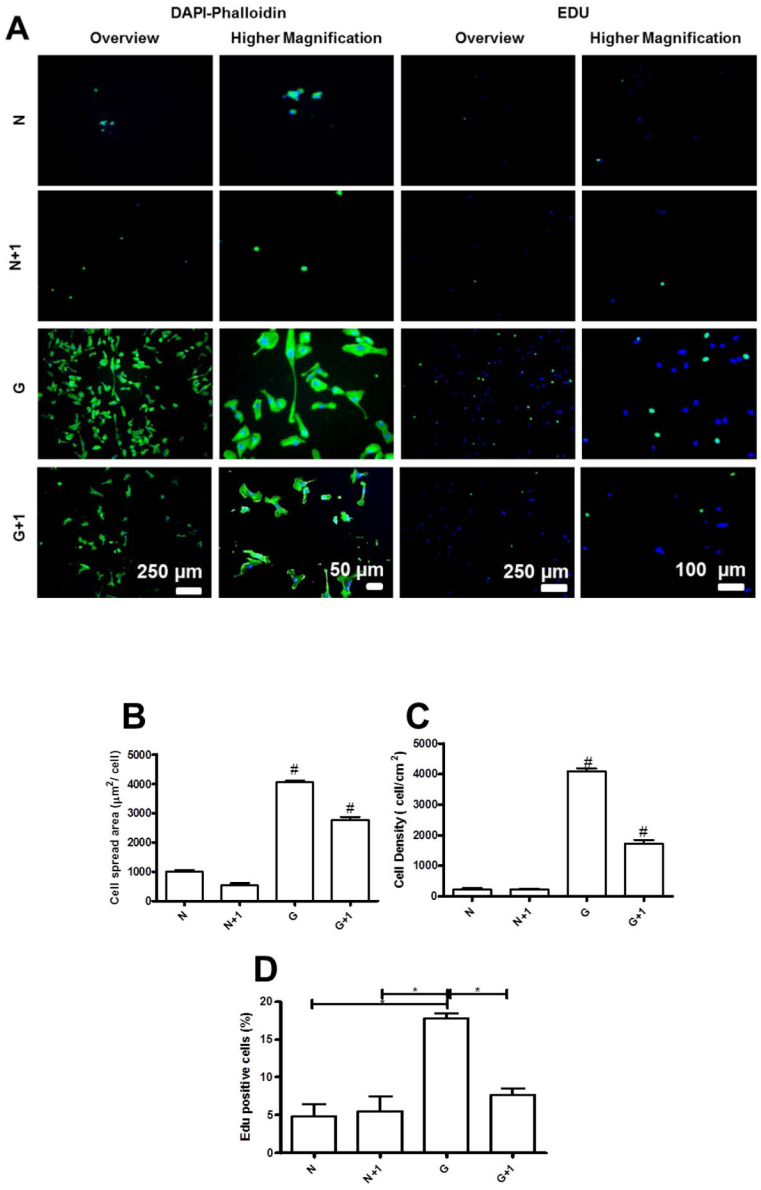

Figure 9.

(A) DAPI/phalloidin staining and representative images of EDU assay for HUVECs adhered on native films (N) and cross-linked films (G) with an additional bilayer on the top of the film and in the presence or absence of adsorbed or immobilized proteins. Quantification of (B) Cell number per field, (C) Cell spread area, and (D) Cell circularity. (E) Percentage of proliferating cells measured by the EDU assay. Statistical analysis was performed, and data was considered statistically different for p values < 0.05 (*). (#) denotes significant differences when compared to all PEMs formulations.

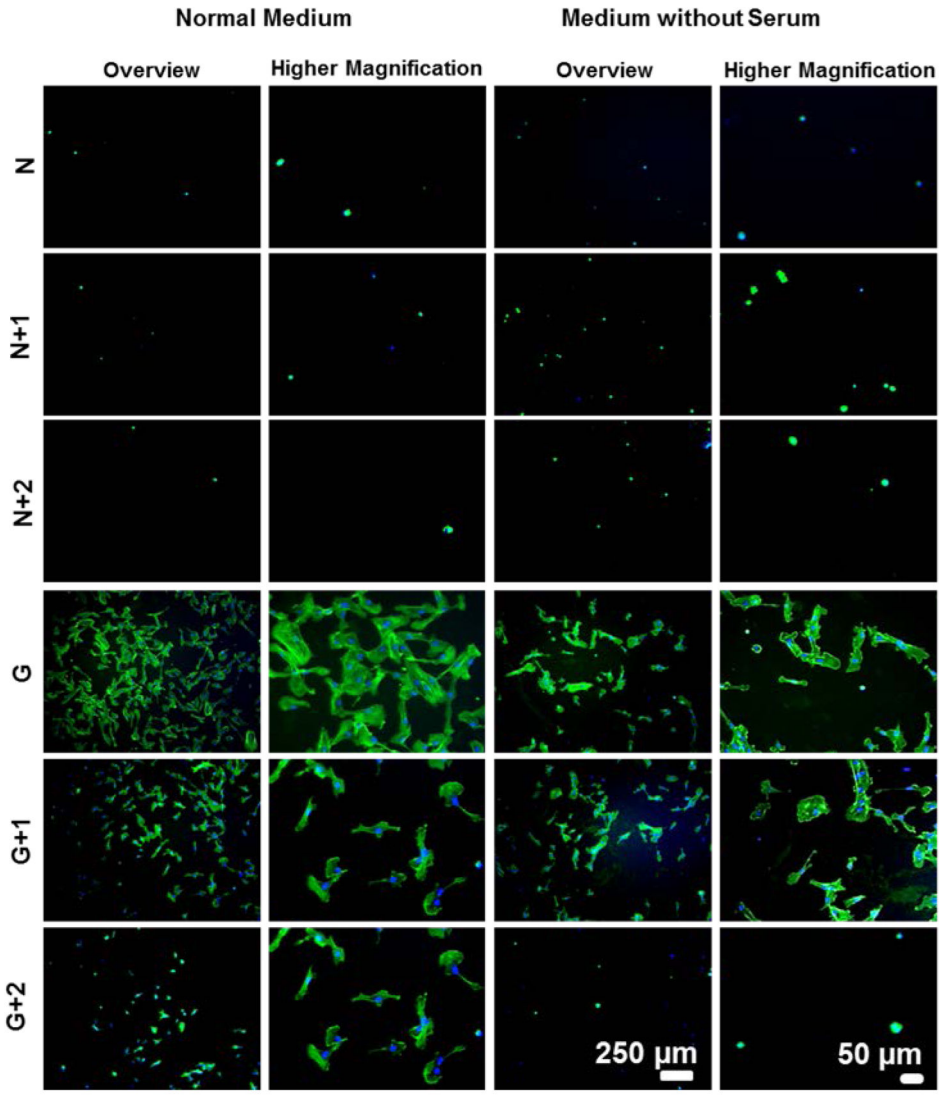

Figure 10.

Adhesion of HUVECS on native (N) and cross-linked films (G) with or without additional bilayers on the top when resuspended in normal medium or medium without serum. Cells nuclei were stained blue by DAPI and F-actin filaments in green by phalloidin.

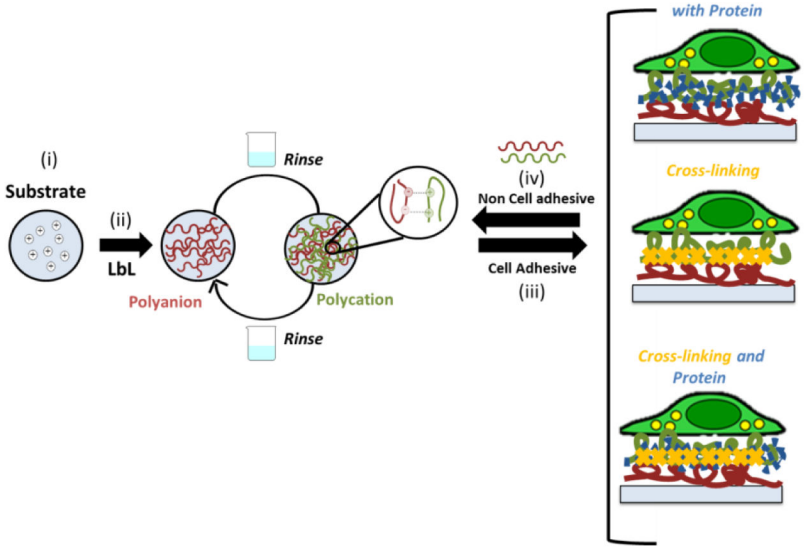

Scheme I.

Schematic representation of layer-by-layer (LbL) adsorption of polyelectrolytes based on electrostatic interactions. (i) The substrate (polystyrene well plates) was first modified with polyethylenimine (PEI) and extensive washed. (ii) The positive charged substrate was coated with polysaccharides that shared marine origin (ALG and CHI) using LbL assembly. Between the polyelectrolyte depositions a washing step was performed. (iii) The adhesive properties of ALG/CHI multilayers can be tuned by the addition of ECM proteins, chemical cross-linking or a combination of thereof. (iv) Upon the addition of ALG/CHI on the top of the cell adhesive ALG/CHI multilayers the films became non-adhesive.